

Disorder-controlled superconductivity at YBa₂Cu₃O₇/SrTiO₃ interfacesJ. Garcia-Barriocanal,¹ A. M. Perez-Muñoz,^{1,2} Z. Sefrioui,¹ D. Arias,^{1,3} M. Varela,^{1,4} C. Leon,¹ S. J. Pennycook,⁴ and J. Santamaria¹¹*GFMC. Dpto. Fisica Aplicada III, Universidad Complutense de Madrid, 28040 Madrid, Spain*²*CEI Campus Moncloa, UCM-UPM, 28040 Madrid, Spain*³*Grupo de Materiales Magnéticos y Nanoestructuras, Universidad del Quindío, Armenia, Spain*⁴*Materials Science & Technology Division, Oak Ridge National Laboratory Oak Ridge, TN 37831-6030, USA*

(Received 30 April 2013; revised manuscript received 23 May 2013; published 11 June 2013)

We examine the effect of interface disorder in suppressing superconductivity in coherently grown ultrathin YBa₂Cu₃O₇ (YBCO) layers on SrTiO₃ (STO) in YBCO/STO superlattices. The termination plane of the STO is TiO₂ and the CuO chains are missing at the interface. Disorder (steps) at the STO interface cause alterations of the stacking sequence of the intracell YBCO atomic layers. Stacking faults give rise to antiphase boundaries which break the continuity of the CuO₂ planes and depress superconductivity. We show that superconductivity is directly controlled by interface disorder outlining the importance of pair breaking and localization by disorder in ultrathin layers.

DOI: [10.1103/PhysRevB.87.245105](https://doi.org/10.1103/PhysRevB.87.245105)

PACS number(s): 74.72.-h, 73.40.-c, 74.78.Fk

Complex oxide interfaces in epitaxial heterostructures have become a very active research area. The thrust of this rapidly expanding field comes partly from the plethora of novel effects and physical phenomena discovered in oxide superlattices and partly by an exciting horizon of novel devices and applications. The electronic reconstruction taking place at these interfaces is known to have important effects triggering modifications of fundamental electronic parameters such as charge density, on site Coulomb interaction and bandwidth giving rise to stabilization of novel electronic ground states with emerging properties.^{1,2} Apart from its fundamental interest, the possibility of tailoring the electronic structure of the interfaces to display novel behaviors and functionalities may open interesting pathways in device design for oxide electronics. Although progress has been made in achieving atomic precision of the interface growth, epitaxial strain, intermixing, or more sophisticated electronic processes related to the polar nature of complex oxides play a role in generating chemical or physical disorder, which may cause profound changes in the free carrier density or other physical quantities controlling the equilibrium between phases.

Devices based on oxide-oxide interfaces, including Schottky and p-n junctions³⁻⁶ and field-effect transistors (FETs)^{7,8} are being extensively investigated. Significant progress has been achieved in the field-effect control of the carrier density of a superconducting cuprate using a FET device⁹ and more recently using electric double layer (EDL) techniques.¹⁰ Electrostatic doping constitutes an alternative to chemical doping with the advantage of not introducing the disorder associated to element substitution. However, in FET devices there is an inherent class of disorder related to an unavoidable presence of an interface which may also deeply influence the doping process. The modulation of the charge density occurs within the Thomas-Fermi screening length, typically of the order of 1 nm. Electrostatic doping is an interfacial phenomenon, and may be influenced by the kinds of interface effects such as strain, charge transfer, polarity mismatch, etc. Moreover, the two-dimensional (2D) character of the cuprate makes its normal and superconducting states especially sensitive to disorder and localization effects which may reduce both the normal

carrier and the superfluid density. In the case of FET devices, the interface between SrTiO₃ (STO) and a superconducting cuprate (often of the 123 family) is of special relevance. These devices exploit the large permittivity values of the STO at low temperatures to achieve an electrostatic modulation of the carrier density of the cuprate by controlling the electric field applied through the gate insulator (STO). But intriguingly, although the critical temperature of the cuprates has been successfully modified in FET experiments, the expected levels of electrostatic doping have never been achieved.^{7,9,11} In the case of EDL transistors, the doping process takes place at the sample surface and thus interface effects between the substrate material and the epitaxial thin film do not affect the electrostatic gating process itself. However, interface disorder plays a role in setting a minimum value in the thickness layer of the cuprate to be doped. Recently Leng *et al.* reports on the appearance of a 5–6 unit cell dead layer in thin YBa₂Cu₃O₇ samples grown on STO substrates.^{12,13} The dead layer has an insulating behavior and as a result, obtaining the clean 2D superconductor, which would play a decisive role in the quantitative analysis of the results obtained with the EDL technique, remains elusive. Identifying interface disorder and its effect on superconductivity suppression are thus of utmost importance for a quantitative interpretation of electrostatic doping experiments.

In this paper we report on the structure and transport properties of YBCO/STO interfaces in epitaxial superlattices with values of the individual layer thickness reduced down to one unit cell. Interface disorder is generated by steps in the STO which give rise to deep modifications in the chemistry of the YBCO layers in the form of stacking faults of intracell perovskite blocks. This results in antiphase boundaries which break the continuity of the CuO₂ planes and degrade superconductivity. We show that both the critical temperature and the carrier density of the ultrathin cuprate layers are controlled by interfacial disorder, outlining the importance of carrier localization by interfacial disorder in electrostatic doping experiments based on YBCO/STO heterostructures.

[YBCO_{*m*}/STO_{*n*}]₉ superlattices were grown on STO (100) substrates in a high-pressure (2.9 mbar) pure oxygen sputtering

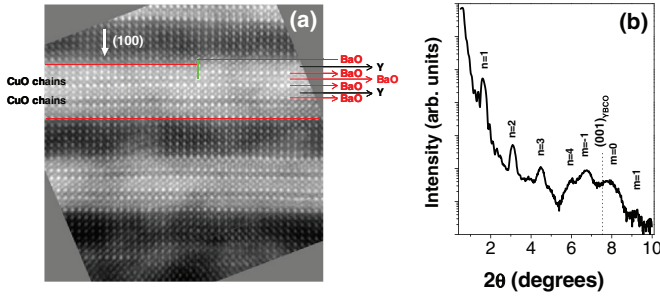


FIG. 1. (Color online) (a) STEM Z-contrast cross-section image of the superlattice $[YBCO_3/STO_6]_9$. The red lines are a guide to the eye to emphasize BaO planes and the heterostructure interface with one STO unit cell step. Black arrows denote Y planes and the green line represents the antiphase boundary. (b) X-ray reflectivity spectrum of the same sample.

system. High pressure and high substrate temperature ($900^\circ C$) ensure a slow (1 nm/min) and highly thermalized growth of complex oxides providing excellent epitaxial properties.^{14,15} Several series of samples were grown with a fixed thickness of STO in 0.8 ($n = 2$ unit cells), 2.4 ($n = 6$ unit cells), and 6 nm ($n = 15$ unit cells) and varying the thickness of the YBCO systematically between 1.2 ($m = 1$ unit cell) and 14 nm ($m = 12$ unit cells). We also grew samples with constant YBCO thickness in 6 nm ($m = 5$ unit cells) and changing the thickness of the STO between 0.4 ($n = 1$ unit cell) and 4 nm ($n = 10$ unit cells). The structure was analyzed by x-ray diffraction (XRD) and it was also probed by scanning transmission electron microscopy (STEM). Z-contrast images were obtained in a VG Microscopes HB501UX STEM operated at 100 kV with a cold field emission gun equipped with a Nion aberration corrector and a Gatan Enfina electron energy loss spectrometer. Cross-section samples for STEM were prepared by conventional grinding, dimpling, and ion milling with Ar ions with an energy of 5 kV, at an incidence angle of 7° . Final cleaning was done at a low voltage of 2 kV.

Both x-ray reflectivity and diffraction and Z-contrast STEM show flat and continuous layers over long lateral distances (see Fig. 1). High-resolution STEM images show the 2D growth of YBCO on STO and coherent interfaces [see Fig. 1(a)]. This is in contrast to the three-dimensional growth reported previously^{16,17} under large compressive strain on $LaAlO_3$ substrates. Figure 1(a) shows a high-resolution image of a $[YBCO_3/STO_6]_9$ superlattice. In the YBCO layers the brighter atomic rows correspond to the heavier Ba and Y planes, while the darker planes correspond to the CuO chains. As shown previously by Matijasevic and co-workers¹⁸ the termination plane of the STO is TiO_2 and the cuprate starts growing with a sequence $(TiO_2)-BaO-CuO_2-Y-CuO_2-BaO-CuO-$, etc. Our Z-contrast images and EELS spectrum images confirm this point. This growth mode is also in agreement with other reports on YBCO single films on TiO_2 -terminated STO substrates.^{19,20} Steps in the STO layer with a height of 1 or 2 unit cells can be readily seen in the STEM image [see Fig. 1(a)]. It is quite remarkable that these steps occur mostly at the top interfaces (sides) of the STO layers, while the bottom interface of the same layer appears flat. In other words, YBCO growth has a flattening effect, as reported previously for YBCO single layers

grown on STO substrates.²⁰ Since the lattice parameter of the STO is about 1/3 of the c -lattice parameter of YBCO, such interface steps induce stacking faults and defective growth of the YBCO layer to end up in a flat surface. Z-contrast images show modified atomic layer sequences in the YBCO associated to the interface steps. Extra $BaO-CuO_2-Y-CuO_2-BaO$ blocks (roughly 0.8 nm thick) are introduced and/or $BaO-CuO-BaO$ blocks (roughly 0.4 nm thick) are removed to compensate the steps. This way, a 2 unit cell step in the STO (0.78 nm in height) can be accommodated including an additional $BaO-CuO_2-Y-CuO_2-BaO$ block, and a 1 unit cell STO step (0.39 nm in height) requires adding a $BaO-CuO_2-Y-CuO_2-BaO$ block and removing a $BaO-CuO-BaO$ unit to end up in a flat YBCO surface. This effect is clearly seen, in the upper YBCO layer of Fig. 1(a). The steps in the STO cause then a layer thickness fluctuation which should be detectable by x-ray reflectivity. Figure 1(b) shows the x-ray reflectivity spectrum of a typical $[STO_6/YBCO_3]_9$ superlattice. The sharp superlattice peaks in a wide angular range (up to 9°) reflect large values of the structural coherence length (>50 nm) as obtained from the full width at medium height of the satellites, showing that structural coherence was limited by sample thickness. The refinement of the reflectivity spectra using the SUPREX 9.0 software²¹ [see Fig. 2(a)], allows quantitative evaluation of the averaged roughness. Figure 2(b) displays roughness values of superlattices with 2, 3, and 5 unit cells of YBCO as a function of the thickness of STO. It is clear that the roughness increases with the thickness of the STO, while it decreases with YBCO thickness, showing that the disorder in the YBCO layer results from the steps in the STO and not the other way around. Furthermore, the roughness increase is less pronounced for thicker YBCO layers, indicating that the step “healing” effect of the stacking faults occurs preferentially in thicker YBCO layers for which the atomic reconstruction at the interface unit cell is less important relative to the YBCO layer volume as a whole. Thus, our structural analysis shows that there is significant chemical disorder being induced in the YBCO layer which may have important consequences for the superconducting properties. Furthermore, carrier density will be modified by the missing CuO chains at the interface (chains

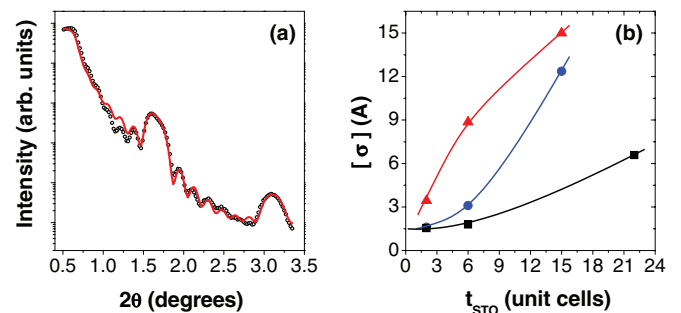


FIG. 2. (Color online) (a) Low angle portion of the reflectivity of the $[YBCO_3/STO_6]_9$ superlattice not affected by overlapping with the finite-size oscillation associated to the (001) YBCO reflection. The line shows the result of the refinement of the reflectivity spectra using the SUPREX 9.0 software. (b) Averaged roughness values obtained from the refinement of superlattices with 2 (triangles), 3 (circles), and 5 (diamonds) unit cells of YBCO as a function of the thickness of STO.

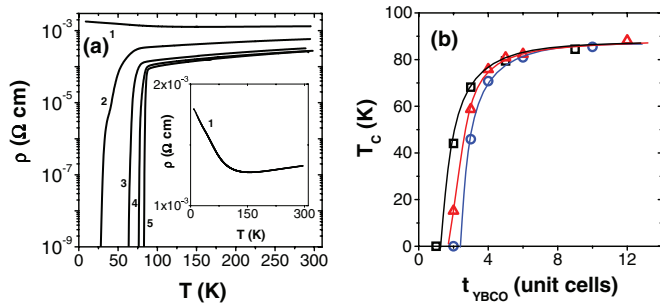


FIG. 3. (Color online) (a) Logarithmic resistance curves of a series of samples with fixed thickness of the STO 0.8 nm (2 unit cells) as a function of the thickness of YBCO. YBCO thickness is 1, 2, 3, 4, and 5 unit cells from top to bottom. Inset: linear resistance plot of a superlattice with 1-unit-cell-thick YBCO layer showing the metallic normal-state resistivity. (b) YBCO thickness dependence of T_C for different thicknesses of the STO spacers. Open squares, 2-unit-cell-thick STO; open triangles, 6-unit-cell-thick STO; open circles, 15-unit-cell-thick STO. Note that the samples which are not superconducting above 8 K are represented with a T_C of 0 K to complete the picture. Solid lines are guides for the eye.

are the charge reservoir) and by intracell reconstruction at the STO steps.

Next we show transport measurements of the superlattices to address the effect of the disorder in the YBCO layer on the superconducting properties. Figure 3(a) shows resistivity curves of a series of samples with a fixed STO thickness of 0.8 nm (2 unit cells) as a function of YBCO thickness. The first observation is that superlattices with 1 unit cell YBCO are not superconducting. Interestingly, the normal-state resistivity displays a metallic behavior (decreases linearly with temperature) and shows a metal-insulator transition at about 150 K [see inset of Fig. 3(a)]. This is a striking result in view of the missing CuO chains and shows that the STO/YBCO interface might provide a different source of doping. In fact, recent theoretical works have proposed that the YBCO cell at the interface may be overdoped by the 0.5 hole per plane being transferred to avoid the polarization catastrophe resulting from polarity mismatch at the $(\text{TiO}_2)^0/(\text{BaO-CuO}_2\text{-Y-CuO}_2)^{-1}$ interface.^{22,23} The metal-to-insulator transition at 150 K points to the importance of interface or intralayer disorder in localizing charge carriers in such ultrathin layers. Figure 3(a) evidences a rapid recovery of the critical temperature when the thickness of the YBCO layers is increased, and in fact values of the bulk are attained above 5 unit cells. This also evidences that the observed decrease in T_C with increasing STO thickness is not due to a lack of oxygenation in YBCO layers, since a value close to $T_C = 90$ K is recovered for sufficiently thick YBCO independently of the STO thickness. Figure 3(b) illustrates the T_C dependence with YBCO thickness for different thicknesses of the STO spacers. Note that the decrease of the critical temperature observed when reducing the YBCO thickness is very sensitive to the STO thickness. It is well established that T_C of single YBCO layers decreases with decreasing its thickness towards the 1 unit cell limit as shown previously on YBCO/PrBa₂Cu₃O₇ (PBCO) heterostructures.^{24,25} In those samples T_C was only determined by the YBCO thickness since interfacial disorder was almost absent, and thus T_C was

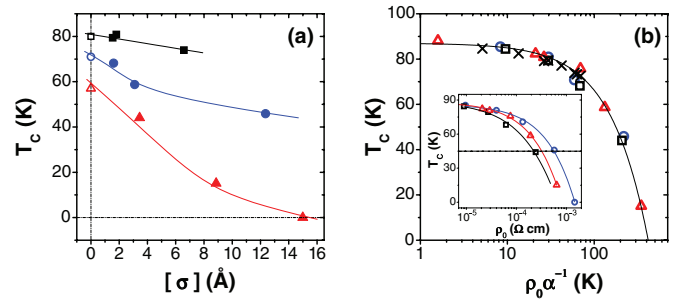


FIG. 4. (Color online) (a) Dependence of the critical temperature on the averaged roughness as determined from SUPREX refinement for superlattices with 2 (triangles), 3 (circles), and 5 (squares) unit cells of YBCO. The open symbols correspond to YBCO/PBCO superlattices with the same YBCO thickness and 5 unit cells of PBCO. These data are represented with $\sigma = 0$ since PBCO has the same structure as YBCO and the interface is essentially flat. (b) T_C as a function of the disorder parameter ρ_0/α for all samples of this study: superlattices with 2-unit-cell-thick STO (open squares), with 6-unit-cell-thick STO (open triangles), and with 15-unit-cell-thick STO (open circles). Crosses correspond to samples with fixed YBCO thickness (5 unit cells). Inset: T_C versus residual resistivity for superlattices with 2-unit-cell-thick STO (open squares), with 6-unit-cell-thick STO (open triangles), and with 15-unit-cell-thick STO (open circles). The dotted line joins samples with the same T_C and disorder (ρ_0/α). Solid lines in the figure are guides for the eye.

found to be independent of PBCO thickness. In YBCO/STO superlattices we observe that, in addition, there is a strong dependence of T_C on the disorder induced by the different STO thickness. For instance, 2 unit cell YBCO layers are superconducting with a $T_C = 44$ K (zero resistance criterion in a linear scale) when the STO spacer is 2 unit cells thick, T_C becomes 15 K when STO thickness is 6 unit cells, and they are nonsuperconducting when STO is 15 unit cells thick. This behavior evidences that the superconducting properties are controlled by the disorder at the YBCO/STO interface. Figure 4(a) shows that the critical temperature of YBCO layers of a given thickness depends strongly on the disorder induced by the interface steps in the STO. The “zero disorder T_C ” ($\sigma \approx 0$) can be estimated from YBCO/PBCO superlattices (open symbols) with the same (2, 3, and 5 unit cells) YBCO thickness.

Figure 4(a) also shows that the effect of disorder is more pronounced in thinner samples, as expected, since disorder-induced localization should be enhanced in 2D. The linear normal-state resistivity curves of Fig. 3(a) allow one to obtain an electrical measure of disorder in terms of the residual resistivity ρ_0 (the 0 K extrapolation of the normal-state resistivity). Thinking in terms of the Matthiessen rule, the ratio ρ_0/α of the residual resistivity over the slope, $\alpha = d\rho/dT$, of the normal-state resistivity-temperature curve, is independent of the number of carriers. Thus, ρ_0/α is as a measure of the (electronic) disorder of the YBCO layer and can be considered as a pair breaking parameter as done previously^{26,27} in ion irradiated YBCO thin films. Interestingly enough, when T_C is plotted as a function of ρ_0/α , all data collapse onto the same line [see Fig. 4(b)], indicating that superconductivity is in fact controlled by disorder. T_C is determined by the number of carriers and by disorder through its effect on pair breaking and

localization.^{28,29} Our result then may suggest that either the number of carriers is constant from sample to sample (which is very unlikely in view of the drastic changes in the chemistry with STO thickness) or it is changing in a way that is also controlled by disorder. In fact the inset of Fig. 4(b) shows the behavior of the residual resistivity ρ_0 as a function of YBCO thickness. The dotted line shows that samples with the same T_C and thus with the same (electronic) disorder ρ_0/α may have different ρ_0 indicating that the carrier density is in fact different.

The picture emerges that the disorder induced by the STO steps affects both the free carrier density and the superfluid density which ultimately determines T_C .³⁰⁻³² Since we find that samples with the same T_C may have different carrier density [see data of the inset of Fig. 4(b) joined at the dotted line], the proportionality between free carrier density and T_C suggested recently³¹ seems not to hold in our case. The effect of disorder goes beyond carrier localization, which would only affect free carrier density, and reduces the number of paired (free) holes more effectively than the number of free holes. This conclusion would imply that although free and paired holes are likely to be related,³⁰ they are not necessarily identical through the pair breaking effect of disorder.

In summary we have shown that in the coherent growth of YBCO on STO disorder in the form steps at the STO surface cause alterations of the stacking sequence of the intracell YBCO atomic layers, which breaks the continuity of the CuO₂ planes and suppresses superconductivity. The intralayer disorder has an effect on carrier localization and pair breaking yielding changes in the ratio of paired over free holes. This result is relevant for electrostatic doping experiments as it provides an explanation for the presence of a dead layer in YBCO ultrathin films grown on STO as well as for localization effects of the injected holes in FET devices based in these heterostructures.

We acknowledge financial support by Spanish MINECO through Grants No. MAT2011-27470-C02 and Consolider Ingenio 2010 No. CSD2009-00013 (Imagine), and the World Wide Materials Program, by CAM through Grant No. S2009/MAT-1756 (Phama), and by the ERC starting Investigator Award, Grant No. 239739 STEMOX (GSS). Research at Oak Ridge National Laboratory was sponsored by the US Department of Energy, Basic Energy Sciences, Materials Sciences and Engineering Division. J.G.B. acknowledges financial support through the Ramon y Cajal Program.

-
- ¹J. Mannhart and D. G. Schlom, *Science* **327**, 1607 (2010).
²H. Y. Hwang, Y. Iwasa, M. Kawasaki, B. Keimer, N. Nagaosa, and Y. Tokura, *Nat. Mater.* **11**, 103 (2012).
³M. Nakamura, A. Sawa, J. Fujioka, M. Kawasaki, and Y. Tokura, *Phys. Rev. B* **82**, 201101(R) (2010).
⁴T. Yajima, Y. Hikita, and H. Y. Hwang, *Nat. Mater.* **10**, 198 (2011).
⁵W. Ramadan, S. B. Ogale, S. Dhar, L. F. Fu, S. R. Shinde, D. C. Kundaliya, M. S. R. Rao, N. D. Browning, and T. Venkatesan, *Phys. Rev. B* **72**, 205333 (2005).
⁶W. Ramadan, S. B. Ogale, S. Dhar, L. F. Fu, N. D. Browning, and T. Venkatesan, *J. Appl. Phys.* **99**, 043906 (2006).
⁷C. H. Ahn, J. M. Triscone, and J. Mannhart, *Nature (London)* **424**, 1015 (2003).
⁸C. H. Ahn, A. Bhattacharya, M. Di Ventura, J. N. Eckstein, C. Daniel Frisbie, M. E. Gershenson, A. M. Goldman, I. H. Inoue, J. Mannhart, Andrew J. Millis, Alberto F. Morpurgo, Douglas Natelson, and Jean-Marc Triscone, *Rev. Mod. Phys.* **78**, 1185 (2006).
⁹J. Mannhart, *Supercond. Sci. Technol.* **9**, 49 (1996).
¹⁰A. T. Bollinger, G. Dubuis, J. Yoon, D. Pavuna, J. Misewich, and I. Bozovic, *Nature (London)* **472**, 458 (2011).
¹¹M. Salluzzo, A. Gambardella, G. M. De Luca, R. Di Capua, Z. Ristic, and R. Vaglio, *Phys. Rev. B* **78**, 054524 (2008).
¹²X. Leng, J. Garcia-Barriocanal, S. Bose, Y. Lee, and A.M. Goldman, *Phys. Rev. Lett.* **107**, 027001 (2011).
¹³X. Leng, J. Garcia-Barriocanal, B. Yang, Y. Lee, J. Kinney, and A.M. Goldman, *Phys. Rev. Lett.* **108**, 067004 (2012).
¹⁴M. Varela, W. Grogger, D. Arias, Z. Sefrioui, C. León, C. Ballesteros, K. M. Krishnan, and J. Santamaría, *Phys. Rev. Lett.* **86**, 5156 (2001).
¹⁵Z. Sefrioui, D. Arias, V. Peña, J. E. Villegas, M. Varela, P. Prieto, C. León, J. L. Martinez, and J. Santamaria, *Phys. Rev. B* **67**, 214511 (2003).
¹⁶L. Ryen, E. Olsson, C. N. L. Edvardsson, and U. Helmerson, *Physica C* **304**, 307 (1998).
¹⁷C. N. L. Edvardsson, U. Helmerson, L. D. Madsen, S. Czigany, L. Ryen, and E. Olsson, *Physica C* **304**, 245 (1998).
¹⁸V. C. Matijasevic, B. Ilge, B. Stäuble-Pümpin, G. Rietveld, F. Tuinstra, and J. E. Mooij, *Phys. Rev. Lett.* **76**, 4765 (1996).
¹⁹S. Bals, G. Rijnders, D. H. A. Blank, and G. van Tendeloo, *Physica C* **355**, 225 (2001).
²⁰G. Rijnders, S. Currás, M. Huijben, D. H. A. Blank, and H. Rogalla, *Appl. Phys. Lett.* **84**, 1150 (2004).
²¹I. K. Schuller, *Phys. Rev. Lett.* **44**, 1597 (1980); W. Sevenhans, M. Gijs, Y. Bruynseraede, H. Homma, and I. K. Schuller, *Phys. Rev. B* **34**, 5955 (1986); E. E. Fullerton, I. K. Schuller, H. Vanderstraeten, and Y. Bruynseraede, *ibid.* **45**, 9292 (1992); D. M. Kelly, E. E. Fullerton, J. Santamaria, and I. K. Schuller, *Scr. Metall. Mater.* **33**, 1603 (1995).
²²N. Pavlenko, I. Elfimov, T. Kopp, and G. A. Sawatzky, *Phys. Rev. B* **75**, 140512(R) (2007).
²³N. Pavlenko and T. Kopp, *Phys. Rev. B* **72**, 174516 (2005).
²⁴M. Varela, Z. Sefrioui, D. Arias, M. A. Navacerrada, M. Lucía, M. A. López de la Torre, C. León, G. D. Loos, F. Sánchez-Quesada, and J. Santamaría, *Phys. Rev. Lett.* **83**, 3936 (1999).
²⁵M. Varela, D. Arias, Z. Sefrioui, C. León, C. Ballesteros, and J. Santamaría, *Phys. Rev. B* **62**, 12509 (2000).
²⁶S. K. Tolpygo, J. Y. Lin, Michael Gurvitch, S. Y. Hou, and J. M. Phillips, *Phys. Rev. B* **53**, 12454 (1996).
²⁷D. Arias, Z. Sefrioui, G. D. Loos, F. Agullo-Rueda, J. Garcia-Barriocanal, C. Leon, and J. Santamaria, *Phys. Rev. B* **68**, 094515 (2003).
²⁸A. M. Goldman and N. Markovic, *Phys. Today* **51** (11), 39 (1998).
²⁹N. Marković, C. Christiansen, and A. M. Goldman, *Phys. Rev. Lett.* **81**, 5217 (1998).
³⁰A. Rüfenacht, J. P. Locquet, J. Fompeyrine, D. Caimi, and P. Martinoli, *Phys. Rev. Lett.* **96**, 227002 (2006).
³¹D. Matthey, N. Reyren, J.-M. Triscone, and T. Schneider, *Phys. Rev. Lett.* **98**, 057002 (2007).
³²Y. J. Uemura *et al.*, *Phys. Rev. Lett.* **62**, 2317 (1989).